MOLECULAR PHYSICS, 2001, VOL. 99, NO. 19, 1669–1678

# Overtone spectrum and the Fermi resonance of the SiH chromophore in $SiHCl_3$

YUN DING*, SHENG-GUI HE, JING-JING ZHENG, SHUI-MING HU, XIANG-HUAI WANG and QING-SHI ZHU

Open Research Laboratory of Bond Selective Chemistry and the Institute for Advanced Studies, University of Science and Technology of China, Hefei 230026, PR China

(*Received 27 February 2001; revised version accepted 8 May 2001*)

The Fourier transform and Fourier transform intracavity laser absorption spectra of the gas phase $SiHCl_3$ molecule were recorded from 1000 $cm^{-1}$ up to 13 000 $cm^{-1}$. The normal mode analysis is carried out to fit the observed band centres. The reduced Hamiltonian models in terms of normal and curvilinear internal coordinates are used to study the Fermi resonance between the SiH stretching and bending modes and analyse the observed band centres associated with the SiH chromophore. The resonance in the SiH chromophore is found not to be important due to the cancellation of the contributions from the kinetic and the potential coupling terms. Off-diagonal anharmonic constants between the SiH stretching and bending manifold and the molecular frame have been determined. The SiH chromophore vibrational intensities are also reported.

## 1. Introduction

Fermi resonances are of central importance for vibrational energy redistribution and intramolecular kinetics [1]. The strong, universal Fermi resonance between the CH stretching and bending modes of $CHX_3$ (X = F [2–7], Cl [8, 9], Br [10, 11], I [12], D [13–18], $CF_3$ [19], etc.) compounds has been widely studied theoretically and experimentally. It is believed to occur universally at the $sp^3$ CH chromophore.

Theoretical interpretation of the Fermi resonance coupling has been of considerable interest. It had been treated by the reduced 3-dimensional (3D) space models in internal curvilinear coordinates [7, 20–25], in normal rectilinear coordinates using a polar coordinate representation of the 3D potential [17, 26], and using other more complex models including all vibrational degrees of freedom [27, 28]. In the first two models it is assumed that the motions of CH stretching and bending can be isolated dynamically from the $CX_3$ frame, and that the strongly anharmonic stretching mode carries substantial oscillator strength at high excitation states (CH chromophore). The assumption has been verified experimentally [3, 26, 29] and in more complete theoretical treatments [27, 28, 30]. The concept of a CH chromophore has been applied successfully to asymmetric [31] and chiral environments [32]. The main difference between the 3D rectilinear normal coordinate and the internal curvilinear coordinate models for the CH chromophore is that in the former the couplings to molecular frame vibrations occurring within the harmonic approximation are considered, whereas in the latter they are not [12]. The normal coordinate model with large Taylor expansion series proposed by Dübal [26] is believed to be the best approximation at the present time. On the other hand, it is believed that the curvilinear internal coordinate description becomes closer to the eigenstate picture as the molecular frame becomes heavier. For the systems where several degrees of freedom may undergo large-amplitude displacements, curvilinear internal coordinates are suggested.

The SiH chromophore in $SiHX_3$ is expected to be similar to the CH chromophore in $CHX_3$, because the two types of molecule present the same geometrical structure. $SiHD_3$ and $SiHF_3$ have been studied [34, 35] and, contrary to the CH chromophore in $CHX_3$ molecules, the Fermi resonance between the SiH stretching and bending modes was found not to be significant. However, this trend is due to the cancellation of the contributions from the kinetic and the potential energy coupling terms. In this paper we study the Fermi resonance in $SiHCl_3$, extending some earlier work. The fundamental spectra have been reported by Bürger and Ruff [36]. The sixth overtone of the SiH stretching was studied by Campargue *et al.* [37] using intracavity laser absorption spectroscopy.

* Author for correspondence. e-mail: dinghai@mail.ustc.edu.cn

*Molecular Physics* ISSN 0026–8976 print/ISSN 1362–3028 online © 2001 Taylor & Francis Ltd
http://www.tandf.co.uk/journals
DOI: 10.1080/00268970110063926

We are reporting here for the first time the vibrational spectra of $SiHCl_3$ from the first up to the fifth overtone of the SiH stretching mode.

## 2. Experimental

### 2.1. *Fourier transform spectroscopy*

The $SiHCl_3$ sample was purchased from Tokyo Kasei Organic Chemical Institute in Japan and used without further purification. The spectra from 1000 $cm^{-1}$ to 12 000 $cm^{-1}$ were recorded with a Bruker IFS 120HR Fourier transform spectrometer which was equipped with a path length adjustable multi-pass gas cell. The maximum optical path length is 123 m.

Because the spectra in which we are interested cover a wide range and because the absorption intensities vary by several orders of magnitude, we used different experimental conditions to record the FT spectra, as listed in table 1. A selection of spectra associated with transitions in the SiH chromophore are presented in figure 1. The pressures were measured with a manometer over the range 0–10 000 Pa. All the spectra were observed at room temperature, which varied from 22.2 °C to 24.0 °C during the measurement.

The absolute intensities associated with the SiH chromophore excitation were also measured in the experiment. The band intensities were obtained by direct integration:

$$I(\nu_0) = \int_{\nu_0-\nu_L}^{\nu_0+\nu_H} -\ln[S(\nu)/S_0(\nu)]\,d\nu/PL. \qquad (1)$$

Here $\nu_0$ is the band centre, $\nu_L$ and $\nu_H$ are the appropriate values for the integral limits, $S(\nu)$ and $S_0(\nu)$ are the transmittance and baseline spectra, respectively, $P$ is the sample pressure and $L$ is the absorption path length. $\nu_L$ and $\nu_H$ are chosen such that the hot band is included. Thus the band intensities are the sum of the cold and hot bands.

### 2.2. *$6\nu_1$ band with Fourier transform intracavity laser absorption spectroscopy*

Fourier transform intracavity laser absorption spectroscopy (FT-ICLAS) was used to record the $6\nu_1$ band located around 12 514 $cm^{-1}$ with the resolution of 0.2 $cm^{-1}$. Here $\nu_1$ is the SiH stretching mode. An 85 cm long absorption cell was placed inside a 151 cm long Ti:sapphire laser cavity. The sample cell was filled with a 14 kPa $SiHCl_3$ sample. The interleave rapid-scan method implemented on the Bruker IFS 120HR was used, and the spectra were recorded for generation times ($t_g$) of 30, 40, 50, 60, 70, 80, 90 and 100 μs. A detailed discussion of this experimental set-up can be found in [38] and [39]. The spectrum of $6\nu_1$ for a generation time of 100 μs is shown in figure 2. No further efforts were carried out to exclude atmospheric absorption, and the spectrum was overlapped with atmospheric water absorption lines.

The intensity of $6\nu_1$ was also measured. Figure 3 shows the dependence between the integrated intensity and the generation time. The slope of the fitted line is the integrated intensity in unit time. The band intensity can be obtained using the simplified formula

$$I(\nu_0, t_g) = \int_{\nu_0-\nu_L}^{\nu_0+\nu_H} -\ln[S(\nu, t_g)/S_0(\nu, t_g)]\,d\nu/PL_{eq}. \qquad (2)$$

Here $\nu_0$ is the band centre, $\nu_L$ and $\nu_H$ are the appropriate values for the integral limits, $I(\nu_0, t_g)$, $S(\nu, t_g)$ and $S_0(\nu, t_g)$ are the band intensity, transmittance and baseline spectra, respectively, for the generation time of $t_g$. $P$ is the sample pressure, $L_{eq} = ct_gD/L$ is the equivalent absorption path length, $c$ is the speed of light, $D$ is the optical length of the sample cell, and $L$ is that of the laser cavity. The absorption in two spectra at generation times of 30 μs and 40 μs was very weak, so they were discarded in the fitting and only six data points are presented in figure 3.

Table 1. Different experimental conditions used to record the Fourier transform absorption spectrum of $SiHCl_3$.

| Region or band/$cm^{-1}$ | Gas pressure/Pa | Detector | Length of absorption path/m | Resolution/$cm^{-1}$ |
|---|---|---|---|---|
| 1000–2000 | 9785 | MCT[a] | 15 | 0.5 |
| 2000–8000 | 1563 | InSb[a] | 87 | 0.03 |
| 4000–6000 | 1563 | InSb[a] | 15 | 0.03 |
| 8000–10 000 | 9785 | Ge | 123 | 0.03 |
| 10 000–12 000 | 9785 | Si | 87 | 0.5 |
| $\nu_1$ (2200–2300) | 195 | InSb[a] | 0.1 | 0.5 |
| $\nu_1 + \nu_4$ (3000–4000) | 6821 | InSb[a] | 0.1 | 0.5 |
| $2\nu_2$ (1550–1650) | 190 | InSb[a] | 15 | 0.5 |
| $6\nu_1$ (12 000–13 000)[b] | 1.4E4 | Si | 1.49E4 | 0.2 |

[a] Liquid-nitrogen cooled.
[b] From FT-ICLAS.

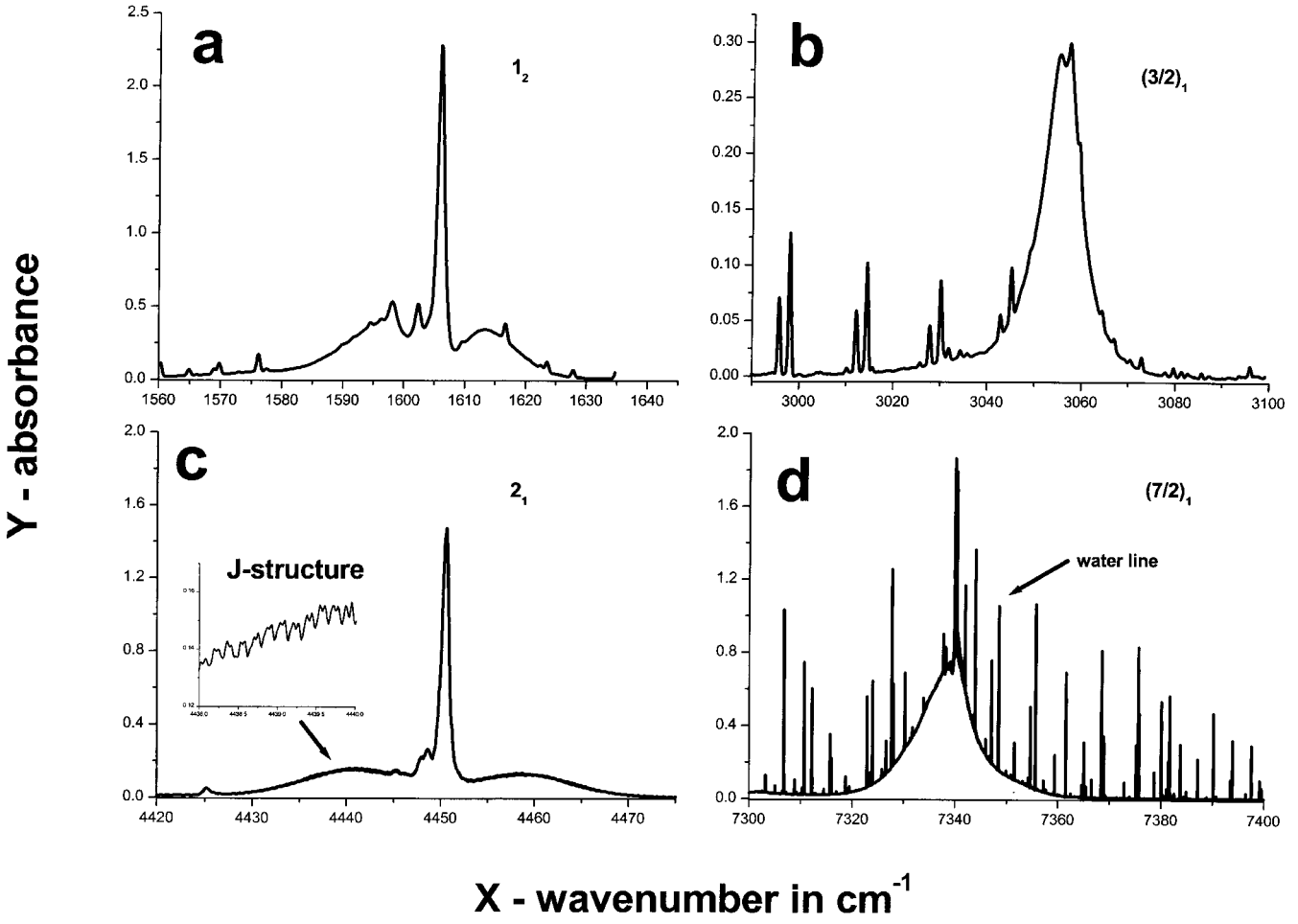


Figure 1. Characteristic absorption bands of the SiH chromophore in $SiHCl_3$ (absorbance $\ln(S_0(\nu)/S(\nu))$). The label of the bands is defined in section 3: (*a*) the $1_2$ band, resolution 0.5 cm$^{-1}$, detector MCT, pressure 190 Pa, absorption path length 15 m; (*b*) the $(3/2)_1$ band, resolution 0.5 cm$^{-1}$, detector InSb, pressure 6821 Pa, absorption path length 10 cm; (*c*) the $2_1$ band, resolution 0.03 cm$^{-1}$, detector InSb, pressure 1565 Pa, absorption path length 15 m; and (*d*) the $(7/2)_1$ band, resolution 0.03 cm$^{-1}$, detector Ge, pressure 9785 Pa, absorption path length 123 m.

### 2.3. *Analysis*

The positions of all the observed transitions are given in table 2, where the assignment is based on a normal mode analysis. Here $\nu_1$ is the SiH stretching vibration, $\nu_2$ is the $SiCl_3$ sym stretch vibration, $\nu_3$ is the $SiCl_3$ 'umbrella' vibration, $\nu_4$ is the SiH bending mode, $\nu_5$ is the $SiCl_3$ deg stretch, and $\nu_6$ is the $SiCl_3$ deg deform. It can be seen from figure 1 that some rotational $J$ structures were resolved in the $n\nu_1$ bands. However, an attempt to analyse them failed due to the complexity originating from the line overlap from $SiH^{35}Cl_3$, $SiH^{35}Cl_2{}^{37}Cl$, and $SiH^{35}Cl^{37}Cl_2$. Therefore the band centres were still obtained directly from the overall band shape. The uncertainty is about 1 cm$^{-1}$ for the strong bands and 2 cm$^{-1}$ for some weak bands. Four hot bands, $n\nu_1 + \nu_4 - \nu_4 (n = 1, 2, 3, \text{and } 4)$ are observed. Their intensities are about 1% of the corresponding value for the cold bands, which agree with the result of estimated calculation.

The intensity uncertainties originate from five main sources: (1) the baseline uncertainty; (2) the band overlapping; (3) the molecule density uncertainty, which comes from the pressure, the temperature, and the absorption path length uncertainties; (4) the limited signal-to-noise ratio (SNR); and (5) the nonlinear response of the instruments (for example, the detector) to the light intensity at a specific frequency. In the experiment some bands were overlapped with $H_2O$ and HCl absorption. In this case the contribution of the water lines to the intensity was deleted by calibrating the water line intensity in the high resolution spectra (0.03 cm$^{-1}$) with the ones listed in Hitran96 database

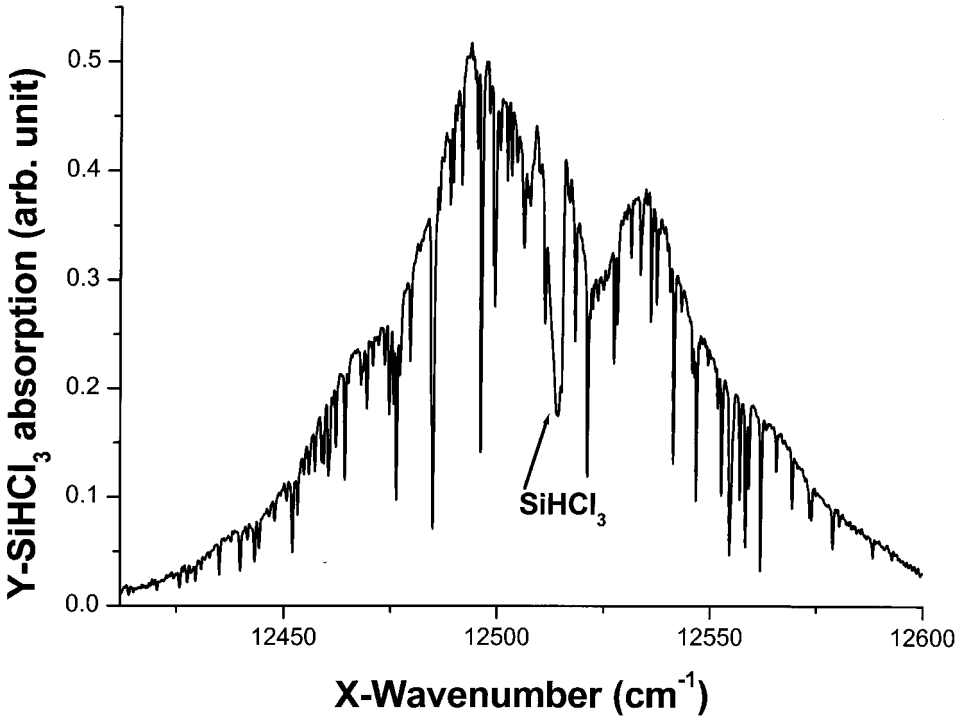


Figure 2. Absorption spectrum of $6\nu_1$ in $SiHCl_3$ recorded by FT-ICLAS. The generation time $t_g$ is 100 μs. The equivalent absorption path length is 16.86 km. The other absorption lines are water lines.

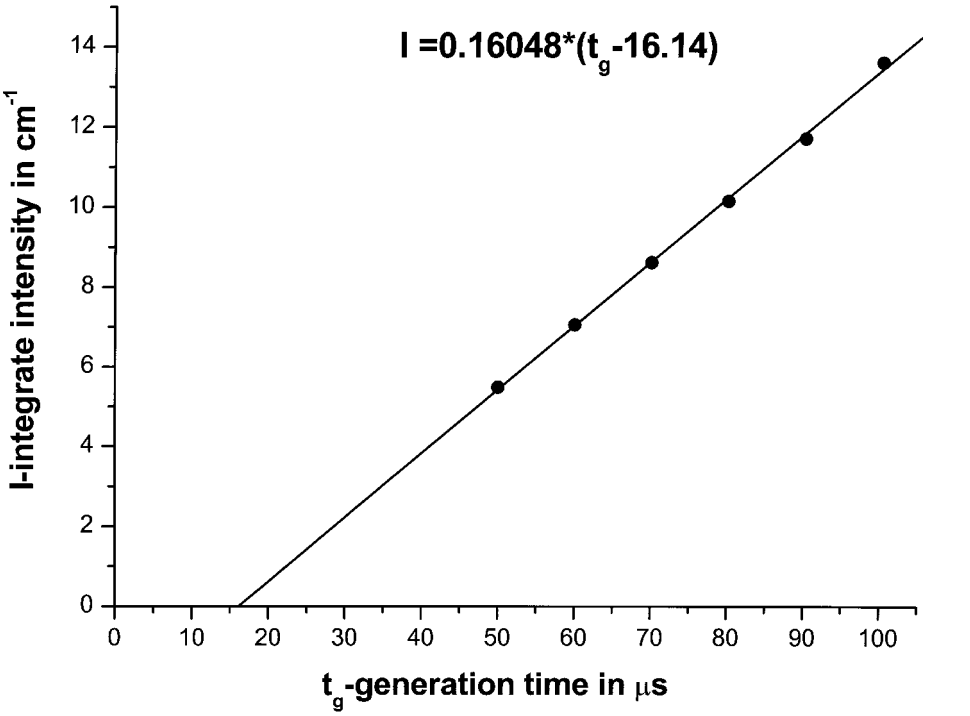


Figure 3. Experimental integrated intensity of the $6\nu_1$ band at different generation times. The slope is the integrated intensity in unit generation time.

[40]. The HCl contribution was subtracted directly. As discussed in [41], we estimate that the absolute intensity uncertainty is around 30% for strong bands and larger for weak bands.

The intensities are given in table 3. It is interesting to note that the $2\nu_1$ band is abnormally weak, about 400 and 15 times weaker than the $\nu_1$ and the $\nu_1 + \nu_4$ bands, respectively. This phenomenon is also observed in

Table 2. Observed band centres in $SiHCl_3$ (in $cm^{-1}$).[a]

| $\tilde{\nu}_{obs}$ | Assignment | Comments | $\tilde{\nu}_{obs}$ | Assignment | Comments |
|---|---|---|---|---|---|
| *175.5[b] | $\nu_6$ | | 2854.0 | $\nu_1+\nu_5$ | |
| *253.7[b] | $\nu_3$ | | 2923.8 | | |
| *498.6[b] | $\nu_2$ | | 2964.3 | $\nu_1+\nu_2+\nu_4$ | uncertain |
| *600.1[b] | $\nu_5$ | | *3054.5 | $\nu_1+\nu_4$ | $(3/2)_1$ |
| *810.8[b] | $\nu_4$ | $(1/2)_1$ | *3231.4 | $\nu_1+2\nu_2$ | |
| 1263.7 | $\nu_2+\nu_5+\nu_6$ | | *3842.0 | $\nu_1+2\nu_4$ | $2_2$ |
| *1302.0 | $\nu_2+\nu_4$ | | *4425.2 | $2\nu_1+\nu_4-\nu_4$ | |
| 1346.3 | $2\nu_4-\nu_3$ | uncertain[c] | *4450.4 | $2\nu_1$ | $2_1$ |
| 1405.3 | $\nu_4+\nu_5$ | | *4624.6 | $\nu_1+3\nu_4$ | $(5/2)_2$ |
| *1435.0 | $3\nu_2$ | | *4704.9 | $2\nu_1+\nu_3$ | |
| *1451.3 | $\nu_1-\nu_4$ | | *5050.6 | $2\nu_1+\nu_5$ | |
| 1458.3 | | | *5232.3 | $2\nu_1+\nu_4$ | $(5/2)_2$ |
| *1606.1 | $2\nu_4$ | $1_2$ | 5406.1 | $\nu_1+4\nu_4$ | broad |
| 1657.5 | $\nu_3+\nu_4+\nu_5$ | uncertain | *6004.6 | $2\nu_1+2\nu_4$ | $3_2$ |
| 1751.3 | $\nu_1-\nu_2$ | | *6530.7 | $3\nu_1+\nu_4-\nu_4$ | |
| 1787.3 | $3\nu_5+\nu_2-\nu_2$ | uncertain | *6570.8 | $3\nu_1$ | $3_1$ |
| *1799.5 | $3\nu_5$ | | *6776.1 | $2\nu_1+3\nu_4$ | $(7/2)_2$ |
| 1901.5 | $3\nu_4-\nu_2$ | broad | *7066.0 | $3\nu_1+\nu_2$ | |
| *2006.5 | $\nu_1-\nu_3$ | | *7170.2 | $3\nu_1+\nu_5$ | |
| 2084.9 | | | *7340.0 | $3\nu_1+\nu_4$ | $(7/2)_1$ |
| *2094.4 | $\nu_2+2\nu_4$ | | *8095.3 | $3\nu_1+2\nu_4$ | $4_2$ |
| *2248.0 | $\nu_1+\nu_4-\nu_4$ | | *8569.2 | $4\nu_1+\nu_4-\nu_4$ | |
| *2260.3 | $\nu_1$ | $1_1$ | *8622.0 | $4\nu_1$ | $4_1$ |
| *2406.3 | $3\nu_4$ | $(3/2)_2$ | *9375.7 | $\nu_4+4\nu_1$ | $(9/2)_1$ |
| *2435.5 | $\nu_1+\nu_6$ | | *10 602.5 | $5\nu_1$ | $5_1$ |
| *2514.6 | $\nu_1+\nu_3$ | | *11 342.6 | $5\nu_1+\nu_4$ | $(11/2)_1$ |
| *2757.0 | $\nu_1+\nu_2$ | | *12 513.9 | $6\nu_1$ | $6_1$ |
| 2765.7 | | | *14 355.1[d] | $7\nu_1$ | $7_1$ |
| 2851.0 | | | | | |

[a] The 42 band centres marked with an asterisk are used in the fitting of the parameters in table 4, column 2.
[b] From reference [36].
[c] The band centres labelled 'uncertain' have a large deviation (about 4 or 5 $cm^{-1}$) between the calculation and observation, and they are uncertain in the assignment.
[d] From reference [37].

$SiHF_3$ [35], where the $3\nu_1$ band is abnormally weak. A study of this SiH chromophore intensity will be presented elsewhere.

## 3. Theory and analysis

### 3.1. *Normal coordinate model*

In the normal coordinate model, the observed band centres are analysed with the effective Hamiltonian matrices. The spectroscopic constants are determined by adjusting the parameters in the matrix element. A theoretical estimation of the band centres may be derived from perturbation theory [42], with

$$\tilde{\nu}=\sum_{i=1}^{6}\tilde{\nu}_i' v_i+\sum_{i=1}^{6}\sum_{j=i}^{6}\tilde{x}_{ij}' v_i v_j+\sum_{i=4}^{6}\sum_{j=i}^{6} g_{ij}' l_i l_j, \quad (3)$$

where $\tilde{\nu}_i'$ is the harmonic constant, $\tilde{x}_{ij}'$, $g_{ij}'$ are the anharmonic constants, and $g_{ij}'$ is only for the generate modes. $v$ and $l$ are the vibrational quantum number and the vibrational angular momentum quantum number, respectively. There are six vibrational modes. Modes 1–3 are non-degenerate, and modes 4–6 are doubly degenerate.

As in $CHX_3$ molecules, if the Fermi resonance exists, the overtone spectrum pertaining to the SiH chromophore in $SiHCl_3$ can be treated separately. In this case, theoretical values for transition wavenumbers can be obtained by explicit diagonalization of the effective Hamiltonian matrix with diagonal elements,

$$\tilde{H}_{\nu_s,\nu_b,l_b;\nu_s,\nu_b,l_b}=\tilde{\nu}_s' v_s+\tilde{\nu}_b' v_b+\tilde{x}_{ss}' v_s^2+\tilde{x}_{bb}' v_b^2+\tilde{x}_{sb}' v_s v_b+g_{bb}' l_b^2, \quad (4)$$

and with off-diagonal elements,

$$\tilde{H}_{\nu_s,\nu_b,l_b;(\nu_s-1),(\nu_b+2),l_b}=\tfrac{1}{2}k_{sbb}'\{\tfrac{1}{2}v_s[(v_b+2)^2-l_b^2]\}^{1/2}. \quad (5)$$

The Hamiltonian matrix is block diagonal in the chromophore polyad quantum number $N=v_s+\frac{1}{2}v_b$.

Table 3. Observed and calculated band centres (in $cm^{-1}$) and the observed absolute intensity (in $cm^{-2}$ per mbar) of the SiH chromophore in $SiHCl_3$.

| $N_j$ | $\tilde{\nu}_{exp}$ | $\tilde{\nu}_{nor}$ [a] | $\tilde{\nu}_{int}$ [b] | Intensity[c] | $N_j$ | $\tilde{\nu}_{exp}$ | $\tilde{\nu}_{nor}$ [a] | $\tilde{\nu}_{int}$ [b] | Intensity[c] |
|---|---|---|---|---|---|---|---|---|---|
| $(1/2)_1$ | 810.8[d] | [−1.6] | [−2.2] | | $5_3$ | | 9601.4 | 9600.1 | |
| $1_2$ | 1606.1 | [1.5] | [2.1] | 4.73*E*-3 | $5_2$ | | 10 119.8 | 10 120.6 | |
| $1_1$ | 2260.3 | [−0.1] | [0.0] | 0.14 | $5_1$ | 10 602.5 | [0.1] | [0.1] | 4.15*E*-7 |
| $(3/2)_2$ | 2406.3 | [0.2] | [0.3] | 3.19*E*-5 | $(11/2)_6$ | | 8590.2 | 8553.2 | |
| $(3/2)_1$ | 3054.5 | [1.2] | [0.7] | 5.58*E*-3 | $(11/2)_5$ | | 9212.1 | 9187.3 | |
| $2_3$ | | 3194.6 | 3194.9 | | $(11/2)_4$ | | 9798.3 | 9785.6 | |
| $2_2$ | 3842.0 | [−1.6] | [−1.0] | 1.45*E*-5 | $(11/2)_3$ | | 10 349.0 | 10 344.6 | |
| $2_1$ | 4450.4 | [0.2] | [0.3] | 3.69*E*-4 | $(11/2)_2$ | | 10 864.0 | 10 863.7 | |
| $(5/2)_3$ | | 3983.2 | 3981.8 | | $(11/2)_1$ | 11 342.6 | [0.7] | [0.8] | |
| $(5/2)_2$ | 4624.6 | [1.0] | [0.8] | | $6_7$ | | 9337.2 | 9276.5 | |
| $(5/2)_1$ | 5232.3 | 5232.3 | 5232.0 | 1.60*E*-4 | $6_6$ | | 9955.7 | 9914.7 | |
| $3_4$ | | 4761.1 | 4757.4 | | $6_5$ | | 10 538.5 | 10 516.2 | |
| $3_3$ | | 5400.1 | 5399.6 | | $6_4$ | | 11 085.8 | 11 076.8 | |
| $3_2$ | 6004.6 | [−1.2] | [−0.7] | | $6_3$ | | 11 597.4 | 11 595.9 | |
| $3_1$ | 6570.8 | [0.3] | [0.4] | 1.76*E*-5 | $6_2$ | | 12 073.3 | 12 074.4 | |
| $(7/2)_4$ | | 5539.4 | 5532.1 | | $6_1$ | 12 513.9 | [−0.3] | [−0.3] | 6.81*E*-8[e] |
| $(7/2)_3$ | | 6175.0 | 6172.3 | | $(13/2)_7$ | | 10 084.7 | 10 027.1 | |
| $(7/2)_2$ | 6776.1 | [−1.2] | [−1.6] | 1.09*E*-7 | $(13/2)_6$ | | 10 699.8 | 10 652.2 | |
| $(7/2)_1$ | 7340.0 | [−0.8] | [−0.1] | 8.67*E*-6 | $(13/2)_5$ | | 11 279.2 | 11 249.3 | |
| $4_5$ | | 6307.0 | 6293.2 | | $(13/2)_4$ | | 11 823.0 | 11 808.1 | |
| $4_4$ | | 6939.2 | 6933.4 | | $(13/2)_3$ | | 12 331.2 | 12 326.4 | |
| $4_3$ | | 7425.7 | 7534.7 | | $(13/2)_2$ | | 12 803.7 | 12 803.9 | |
| $4_2$ | 8095.3 | [1.2] | [1.8] | | $(13/2)_1$ | | 13 240.7 | 13 241.1 | |
| $4_1$ | 8622.0 | [−0.2] | [−0.2] | 3.25*E*-6 | $7_8$ | | 10 821.4 | 10 722.8 | |
| $(9/2)_5$ | | 7075.1 | 7056.1 | | $7_7$ | | 11 433.1 | 11 357.0 | |
| $(9/2)_4$ | | 7703.8 | 7693.6 | | $7_6$ | | 12 009.1 | 11 960.4 | |
| $(9/2)_3$ | | 8296.9 | 8293.3 | | $7_5$ | | 12 549.5 | 12 523.6 | |
| $(9/2)_2$ | | 8854.4 | 8853.9 | | $7_4$ | | 13 054.3 | 13 044.2 | |
| $(9/2)_1$ | 9375.7 | [0.5] | [0.3] | 4.56*E*-7 | $7_3$ | | 13 523.4 | 13 522.1 | |
| $5_6$ | | 7832.4 | 7800.1 | | $7_2$ | | 13 956.9 | 13 958.6 | |
| $5_5$ | | 8457.7 | 8439.3 | | $7_1$ | 14 355.1[f] | [−0.3] | [−0.3] | |
| $5_4$ | | 9047.4 | 9039.9 | | | | | | |

[a] Wavenumbers predicted with the effective Hamiltonian derived from the fitting of the observed transition wavenumbers in the SiH chromophore (table 4, column 4), hot bands excluded. The data listed in brackets are calc − obs.
[b] Wavenumbers predicted with internal coordinate model (table 5), hot bands excluded.
[c] All intensities are for $T = 298$ K.
[d] From reference [36].
[e] From FT-ICLAS experiment.
[f] From reference [37].

Here $v_s$, $v_b$, and $l_b$ are the stretching, bending, and vibrational angular momentum quantum numbers ($v_s = v_1$, $v_b = v_4$, and $l_b = l_4$ for $SiHCl_3$), respectively. The seven adjustable parameters, $\tilde{\nu}'_s, \tilde{\nu}'_b, \tilde{x}'_{ss}, \tilde{x}'_{bb}, \tilde{x}'_{sb}, g'_{ll}$ in the conventional spectroscopic notation define the diagonal structure, and $k'_{sbb}$ defines the off-diagonal Fermi resonance coupling. In each $N$ polyad there are $N + 1$ components labelled by the index $j$ in $N_j$. Here the notation used by Dübal and Quack [3] is adopted.

Equation (3) was used for an analysis of the bands not associated with the SiH chromophore. For those associated with the SiH chromophore, equations (4) and (5) were used. The Levenberg–Marquardt algorithm was used in the nonlinear fitting procedure, in which the original perturbation treatment of equation (3) could be obtained by fixing $k'_{sbb}$ to zero. To reduce the sizes of the matrices, the maximum polyad number $N$ was set to 10 and the maximum quantum number for $\nu_4$ was set to 12. Because no band with a high value of $l$ was observed in the experiment, the maximum $l$ was set to one.

The modes pertaining to the SiH chromophore were analysed both within the pure perturbative treatment (setting $k'_{sbb}$ to zero) and within the resonance picture of the effective Hamiltonian. Forty-two band centres marked with '*' in table 2 were used as input in the fitting to give the constants in equation (3). They are listed in column 2 of table 4. The band centres pertaining to the SiH chromophore were used to determine

Table 4. Effective spectroscopic constant of $SiHCl_3$.[a]

| | $Fit_{obs}$[b] | $Fit_{obs}$[c] | $Fit_{obs}$[d] | $Fit_{int}$[e] |
|---|---|---|---|---|
| $\tilde{\nu}_s'$ | 2295.375 (53) | 2295.388 (70) | 2295.119 (85) | 2294.74 (21) |
| $\tilde{\nu}_b'$ | 808.41 (13) | 808.35 (16) | 808.94 (19) | 809.33 (20) |
| $\tilde{x}_{ss}'$ | −34.9585 (92) | −34.962 (12) | −34.919 (15) | −35.000 (39) |
| $\tilde{x}_{sb}'$ | −13.598 (27) | −13.584 (34) | −13.691 (41) | −14.37 (31) |
| $\tilde{x}_{bb}'$ | −2.447 (42) | −2.420 (54) | −2.570 (64) | −2.45 (11) |
| $g_{bb}'$ | 2.816 (90) | 2.69 (12) | 2.80 (14) | 1.81 (19) |
| $k_{sbb}'$ | 0.0[f] | 0.0[f] | 0.0[f] | 27.5 (64) |
| $\tilde{\nu}_2$ | 508.19 (23) | | | |
| $\tilde{\nu}_3$ | 253.86 (13) | | | |
| $\tilde{\nu}_5$ | 600.40 (28) | | | |
| $\tilde{\nu}_6$ | 175.29 (14) | | | |
| $\tilde{x}_{12}'$ | −1.655 (87) | | | |
| $\tilde{x}_{13}'$ | 0.11 (13) | | | |
| $\tilde{x}_{15}'$ | −0.429 (94) | | | |
| $\tilde{x}_{22}'$ | −10.027 (8) | | | |
| $\tilde{x}_{24}'$ | −5.31 (14) | | | |
| $\tilde{x}_{55}'$ | −0.19 (10) | | | |
| RMS[g] | 1.14 | 1.15 | 1.07 | 0.05 |
| $n$[h] | 42 | 24 | 20 | 20 |

[a] All values are in $cm^{-1}$; uncertainties are given in parentheses in the unit of the last significant digit.
[b] Fit to observed transitions, including hot bands and assigned combination bands; data equally weighted.
[c] Fit to observed transitions, SiH chromophore only, including four hot bands, $n\nu_1 + \nu_4 - \nu_4 (n = 1, 2, 3, \text{and } 4)$.
[d] Fit to observed transitions, SiH chromophore only, hot bands excluded.
[e] Fit to calculated transitions from internal coordinate model (table 5); chromophore modes up to polyad $N = 7$, hot bands excluded.
[f] Fixed.
[g] Root mean-square of the fitting residual in $cm^{-1}$.
[h] Number of input data in the fitting

the parameters in equations (4) and (5), which are listed in columns 3 and 4 of table 4. The value of $k_{sbb}'$ within the resonance treatment is very small in a free fitting. It is only about 0.1 $cm^{-1}$, but the uncertainty in $k_{sbb}'$ is very large. Thus, $k_{sbb}'$ could not be determined and was set to zero.

### 3.2. *Curvilinear internal coordinate model*

In the curvilinear internal coordinate model, the motions of the SiH chromophore are denoted as $r, \theta_1$, and $\theta_2$. Here $r$ is the SiH bond length displacement, and $\theta_1$ and $\theta_2$ are the symmetric coordinates for the bending modes:

$$\theta_1 = (2\phi_1 - \phi_2 - \phi_3)/\sqrt{6},$$
$$\theta_2 = (\phi_2 - \phi_3)/\sqrt{2}. \quad (6)$$

Here $\phi_1, \phi_2$, and $\phi_3$ are the displacements of three HSiCl angles from the equilibrium configuration. The vibrational Hamiltonian takes the form [23]:

$$H = T + V, \quad (7)$$

where

$$T = \tfrac{1}{2}g_{rr}p_r^2 + \tfrac{1}{2}g_{\theta\theta}^0 p_\theta^2 + \frac{1}{2\sqrt{6}}g_6(p_+\theta_+p_+ + p_-\theta_-p_-) + \tfrac{1}{24}(g_4 + 2g_5)(p_+\theta_-^2p_+ + p_-\theta_+^2p_-) + \tfrac{1}{24}(2g_4 + g_5 + 3g_7)(p_+\theta_-\theta_+p_- + p_-\theta_-\theta_+p_+) + \tfrac{1}{2}a^{-1}g_1yp_\theta^2 + \tfrac{1}{2}g_2p_r[(\theta_1p_{\theta_1} + \theta_2p_{\theta_2}) + (p_{\theta_1}\theta_1 + p_{\theta_2}\theta_2)] + \tfrac{1}{4}(a^{-2}g_3 + a^{-1}g_1)y^2p_\theta^2, \quad (8)$$

and

$$V = D_e y^2 + \tfrac{1}{2}F_{\theta\theta}\theta^2 + \tfrac{1}{12}F_{\theta\theta\theta}(\theta_+^3 + \theta_-^3) + \tfrac{1}{24}F_{\theta\theta\theta\theta}\theta^4 + \tfrac{1}{2}a^{-1}F_{r\theta\theta}y\theta^2 + \tfrac{1}{4}(a^{-2}F_{rr\theta\theta} + a^{-1}F_{r\theta\theta})y^2\theta^2. \quad (9)$$

In the above equations, $p_r$ is the momentum conjugate to $r$, $p_{\theta_1}$ and $p_{\theta_2}$ are the momenta conjugate to $\theta_1$ and $\theta_2$, respectively, $p_\theta^2 = p_{\theta_1}^2 + p_{\theta_2}^2, p_{\theta_\pm} = p_{\theta_1} \pm ip_{\theta_2}$, and $\theta^2 = \theta_1^2 + \theta_2^2$. The Morse coordinate is denoted as $y = 1 - \exp(-ar)$, where $a$ is the Morse parameter. Explicit expressions for the kinetic energy expansion coefficients $g_{rr}, g_{\theta\theta}^0$, and $g_i (i = 1, 2, \ldots, 7)$ have been described elsewhere [20, 22, 23]. Definitions of the potential energy parameters, $D_e, F_{rr}, F_{\theta\theta}, F_{\theta\theta\theta}, F_{\theta\theta\theta\theta}, F_{r\theta\theta}$, and $F_{rr\theta\theta}$ have also been given explicitly in the original references [20, 22].

Table 5. Kinetic coefficients and optimized potential energy parameters for $SiH^{35}Cl_3$.[a]

| Kinetic[b] | | Potential | |
|---|---|---|---|
| $g_{rr}/u^{-1}$ | 1.028 52 | $D_e$/aJ | 0.780 088[c] |
| $g^0_{\theta\theta}/u^{-1}\text{Å}^{-2}$ | 0.738 148 | $a/\text{Å}^{-1}$ | 1.420 31[c] |
| $g_1/u^{-1}\text{Å}^{-3}$ | −0.988 139 | $\omega/cm^{-1}$ | 2343.95 (53) |
| $g_2/u^{-1}\text{Å}^{-1}$ | 0.005 583 84 | $\omega x/cm^{-1}$ | 34.977 (62) |
| $g_3/u^{-1}\text{Å}^{-4}$ | 2.017 48 | $F_{\theta\theta}$/aJ | 0.537 3 (17) |
| $g_4/u^{-1}\text{Å}^{-2}$ | 0.366 382 | $F_{\theta\theta\theta}$/aJ | 0[d] |
| $g_5/u^{-1}\text{Å}^{-2}$ | −0.638 085 | $F_{\theta\theta\theta\theta}$/aJ | 1.083 (95) |
| $g_6/u^{-1}\text{Å}^{-2}$ | 0.263 245 | $F_{r\theta\theta}/\text{aJ}\,\text{Å}^{-1}$ | −0.341 6 (87) |
| $g_7/u^{-1}\text{Å}^{-2}$ | −0.334 547 | $F_{rr\theta\theta}/\text{aJ}\,\text{Å}^{-2}$ | 0[d] |

[a] Uncertainties are given in parentheses in the last significant digit, u is the atomic mass unit and $1\,\text{aJ} = 10^{-18}\,\text{J}$.
[b] Definitions of the kinetic parameters are given in [20, 22, 23], and the values of bond length and bond angle are taken from [36].
[c] Calculated from $\omega$, $\omega x$.
[d] Constrained to zero, see text for details.

The program used to optimize the potential parameters of $CHI_3$ [33], $SiHD_3$ [34], and $SiHF_3$ [35] was used here for $SiHCl_3$. The basis set in the variational calculations of the eigenvalues of the Hamiltonain is as follows: $n_{max} = 12$, $v_{max} = 30$, $l_{max} = 6$, $E_{max} = 31\,000\,\text{cm}^{-1}$ and $E(\text{bend})_{max} = 23\,000\,\text{cm}^{-1}$ (see [23]). Test calculations indicated that all vibrational levels of interest were converged better than $0.01\,\text{cm}^{-1}$. Twenty cold bands were used for the determination of the poential parameters. The band at $5406.1\,\text{cm}^{-1}$ was discarded in the optimization due to the large experimental uncertainty. The band at $4624.6\,\text{cm}^{-1}$ was given smaller weight (0.5) while all others were unit weighted. To overcome the high correlation between $F_{rr\theta\theta}$ and $F_{r\theta\theta}$, we adopted the method suggested in [23], i.e. to constrain $F_{rr\theta}$ and the whole coeffcients of the $y^2\theta^2$ term in equation (9) to zero. The kinetic coefficients and optimized potential parameters for the SiH chromophore in $SiHCl_3$ are listed in table 5. We optimized the Morse harmonic wavenumber $\omega = (2a\hbar/hc)(g_{rr}D_e/2)^{1/2}$ and the anharmonic para-meter $\omega x = a^2\hbar^2 g_{rr}/(2hc)$ instead of $a$ and $D_e$ because of the smaller correlation between $\omega$ and $\omega x$ than between $a$ and $D_e$. In the fitting, the (roots mean-square) deviation was $1.0\,\text{cm}^{-1}$, which is within the experimental uncertainty.

## 4. Discussion

The calculated and observed SiH chromophore transition wavenumbers both in the normal and the internal coordinate models are listed in table 3. In $SiHF_3$ some bands are perturbed severely and had to be discarded in the fitting or given a lower weight [35]. However, in $SiHCl_3$ the two models give good agreement between the calculation and the observation. All differences between experimental and calculated data are smaller than $2.2\,\text{cm}^{-1}$, which shows that the assumption that the SiH chromophore is dynamically isolated from the $SiCl_3$ frame is reasonable in $SiHCl_3$ molecule.

The predicted transitions up to polyad number $N = 7$ are all listed. The values predicted by the two models are close to each other, especially in low polyads. In high polyads or the band with high bending vibrational quantum number the differences become larger, but the largest difference is still smaller than $100\,\text{cm}^{-1}$. Thus the predictions from the two models are quite consistent and can be useful for further investigations in the high overtone region. The results give good predictions, even for the very high overtones, which accords so well with the data in Ref [43]. All the differences are within $1.5\,\text{cm}^{-1}$.

In table 3, one interesting point is that the agreement of the calculation with the observation for the stretching overtones is better than that for the bending or stretching and bending combinations. The largest deviation for stretching is $0.3\,\text{cm}^{-1}$ in the normal mode model, and $0.4\,\text{cm}^{-1}$ in the internal coordinate model, occurring for $3\nu_1$. The deviation is relatively larger for the bending modes. For example, for $\nu_4$, the deviation is $1.6\,\text{cm}^{-1}$ or $2.1\,\text{cm}^{-1}$; and for $2\nu_4$ it is $1.5\,\text{cm}^{-1}$ or $2.1\,\text{cm}^{-1}$. For the seven pure stretching bands the RMS deviation is only $0.23\,\text{cm}^{-1}$ and $0.26\,\text{cm}^{-1}$, while it is $1.1\,\text{cm}^{-1}$ and $1.2\,\text{cm}^{-1}$ for the rest of the 13 transitions including bending modes in the normal and internal coordinate models, respectively. This showed that probably the bending modes are perturbed by the motions of the $SiCl_3$ frame, e.g. $\nu_5 + \nu_6$ is at $775.6\,\text{cm}^{-1}$, and $\nu_3 + \nu_5$ is at $853.8\,\text{cm}^{-1}$. Both of them are close to

Table 6. Cancellation of the kinetic energy and the potential energy coupling term in some $XHY_3$-type molecules.

| Species | $\frac{g_1}{u^{-1}Å^{-3}}$ | $\frac{F_{r\theta\theta}}{aJÅ^{-1}}$ | $\frac{g^0_{\theta\theta}}{u^{-1}Å^{-2}}$ | $\frac{F_{\theta\theta}}{aJ}$ | $\frac{a}{Å^{-1}}$ | $\frac{\frac{1}{2}a^{-1}F_{r\theta\theta}\alpha_\theta^{-1}}{cm^{-1}}$ | $\frac{\frac{1}{2}a^{-1}g_1\alpha_\theta\hbar^2}{cm^{-1}}$ | $\frac{\text{Difference}}{cm^{-1}}$ |
|---|---|---|---|---|---|---|---|---|
| $CHF_3$[a] | −2.49 | −0.27 | 1.44 | 0.81 | 1.81 | −129.6 | −672.1 | 542.5 |
| $CHCl_3$[a] | −2.46 | −0.38 | 1.39 | 0.89 | 1.88 | −164.5 | −682.0 | 517.5 |
| $CHBr_3$[b] | −2.48 | −0.25 | 1.38 | 0.59 | 1.87 | −133.2 | −564.9 | 431.7 |
| $CHI_3$[c] | −2.52 | −0.13 | 1.39 | 0.50 | 1.86 | −75.9 | −529.3 | 453.4 |
| $SiHD_3$[d] | −0.96 | −0.37 | 0.95 | 0.46 | 1.39 | −249.2 | −313.1 | 63.9 |
| $SiHF_3$[e] | −1.03 | −0.47 | 0.78 | 0.55 | 1.37 | −266.1 | −411.2 | 145.1 |
| $SiHCl_3$[f] | −0.99 | −0.34 | 0.74 | 0.54 | 1.42 | −182.6 | −387.9 | 205.3 |

[a] The data are taken from reference [20]; $\alpha_\theta = (F_{\theta\theta}/g^0_{\theta\theta})^{1/2}/\hbar$.
[b] From reference [11].
[c] From reference [12].
[d] From reference [34].
[e] From reference [35].
[f] From this work.

the $\nu_4$ band which lies at 810.8 $cm^{-1}$. There may exist some resonance between the related upper levels. This point ought to be verified by *ab initio* calculation or using a more refined model with the $SiCl_3$ frame included.

The overtone transition wavenumbers calculated using the potential parameters were also fitted with the effective non-diagonal Hamiltonian. The fitted spectroscopic constants are listed in table 4, column 5. In this fitting, $k'_{sbb}$ is determined as $27.5 \pm 6.4\ cm^{-1}$, compared with the result that $k'_{sbb}$ is nearly zero with a very large uncertainty when using the normal coordinate model to fit the experimental data directly. The RMS deviation changed very little if $k'_{sbb}$ were fixed to zero, and still gave a good description of the calculated spectrum.

All the results show that the Fermi resonance in the SiH chromophore should be small in $SiHCl_3$. The reason for this insignificance of the stretching–bending coupling is due to the cancellation between the kinetic and the potential energy coupling terms [34]. The contributions to Fermi resonsence come mainly from the kinetic energy coupling term, $\frac{1}{2}a^{-1}g_1 y p_\theta^2$, and the potential energy coupling term, $\frac{1}{2}a^{-1}F_{r\theta\theta}y\theta^2$. The corresponding matrix elements are (with the vibrational angular momentum $l = 0$ for simplification):

$$< v_b|\theta^2|v_b + 2 > = +[(v_b + 2)/2]\alpha_\theta^{-1},$$
$$< v_b|p_\theta^2|v_b + 2 > = -[(v_b + 2)/2]\alpha_\theta\hbar^2, \qquad (10)$$

where $\alpha_\theta = (F_{\theta\theta}/g^0_{\theta\theta})^{1/2}/\hbar$. The matrix element contributions from the kinetic and potential energy terms are of opposite sign. In $SiHCl_3$ the value of $\frac{1}{2}a^{-1}F_{r\theta\theta}\alpha_\theta^{-1}$ is $-182.6\ cm^{-1}$ and the value of $\frac{1}{2}a^{-1}g_1\alpha_\theta\hbar^2$ is $-387.9\ cm^{-1}$, and the difference is 205.3 $cm^{-1}$. Some data of other molecules are listed in table 6, and it can be seen that in $SiHCl_3$ the contributions of the matrix element from kinetic and potential terms are comparable, and a significant cancellation occurs. This cancellation is also significant for $SiHD_3$ [34] and $SiHF_3$ [35], where the differences are only 63.9 $cm^{-1}$ and 145.1 $cm^{-1}$, respectively. However, for $CHX_3$ molecules with strong Fermi resonance the cancellation is not significant and the differences are all larger than 400 $cm^{-1}$. Thus, the Fermi resonances involving SiH stretching and bending are not important for $SiHCl_3$. This also implies a slow energy redistribution between the stretching and bending motions [29].

## 5. Conclusion

Vibrational spectra of gas phase $SiHCl_3$ have been reported. The overtone and combination bands have been observed and assigned, and the experimental absolute band intensities estimated. The assumption of an SiH chromophore has been proved to be a good approximation. The spectroscopic constants $\tilde{x}'_{ij}$ between the SiH chromophore and molecular frame vibrations have been determined. The Fermi resonance within the SiH chromophore has been analysed by effective Hamiltonian and internal curvilinear coordinate models. The potential parameters were optimized by fitting the experimental band centres. The insignificance of the Fermi resonance between SiH stretching and bending motions was attributed to a cancellation of the contributions from kinetic and potential terms.

This work was partially supported by the National Project for the Development of Key Fundamental Sciences in China, by the National Natural Science Foundation of China, by the Foundation of Ministry

of Education of China, and by the Foundation of the Chinese Academy of Science.

## References


[1] Intramolecular kinetics, 1983, *Faraday Discuss. chem. Soc.*, **75**.

[2] Dübal, H.-R., and Quack, M., 1981, *Chem. Phys. Lett.*, **80,** 439.

[3] Dübal, H.-R., and Quack, M., 1984, *J. chem. Phys.*, **81,** 3779.

[4] Campargue, A., and Stoeckel, F., 1986, *J. chem. Phys.*, **85,** 1220.

[5] Segall, J., Zare, R. N., Dübal, H.-R., Lewerenz, M., and Quack, M., 1987, *J. chem. Phys.*, **86,** 634.

[6] Wong, J. S., Green, Jr., W. H., Cheng, C.-K., and Moore, C. B., 1987, *J. chem. Phys.*, **86,** 5994.

[7] Green, Jr., W. H., Cheng, C.-K., and Moore, C. B., 1987, *J. chem. Phys.*, **86,** 6000.

[8] Baggott, J. E., Clase, J. H., and Mills, I. M., 1986, *J. chem. Phys.*, **84,** 4193.

[9] Lewerenz, M., and Quack, M., 1986, *Chem. Phys. Lett.*, **123,** 197.

[10] Ross, A. J., Hollenstein, H., Marquardt, R. R., and Quack, M., 1989, *Chem. Phys. Lett.*, **156,** 455.

[11] Davidsson, J., Gutow, J. H., Zare, R. N., Hollenstein, H. A., Marquardt, R. R., and Quack, M., 1991, *J. chem. Phys.*, **95,** 1201.

[12] Marquardt, R., Goncalves, N. S., and Sala, O., 1995, *J. chem. Phys.*, **103,** 8391.

[13] Peyerimhoff, S., Lewerenz, M., and Quack, M., 1984, *Chem. Phys. Lett.*, **109,** 563.

[14] Perry, J. W., Moll, D. J., Kuppermann, A., and Zewail, A., 1985, *J. chem. Phys.*, **82,** 1195.

[15] Campargue, A., Stoeckel, F., Chenevier, M., and Kraiem, H. B., 1987, *J. chem. Phys.*, **87,** 5598.

[16] Kraiem, H. B., Campargue, A., Stoeckel, F., and Chenevier, M., 1989, *J. chem. Phys.*, **91,** 2148.

[17] Lewerenz, M., and Quack, M., 1988, *J. chem. Phys.*, **88,** 5408.

[18] Permogorov, D., Campargue, A., Chenevier, M., and Kraiem, H. B., 1995, *J. molec. Spectrosc.*, **170,** 10.

[19] Baggott, J. E., Chuang, M.-C., Zare, R. N., Dübal, H.-R., and Quack, M., 1985, *J. chem. Phys.*, **82,** 1195.

[20] Kauppi, E., and Halonen, L., 1989, *J. chem. Phys.*, **90,** 6980.

[21] Halonen, L., Carrington, Jr., T., and Quark, M., 1988, *J. chem. Soc. Faraday Transii*, **84,** 1371.

[22] Halonen, L., and Kauppi, E., 1990, *J. chem. Phys.*, **92,** 3278.

[23] Kauppi, E., 1994, *J. molec. Spectrosc.*, **167,** 314.

[24] Kauppi, E., 1994, *J. chem. Phys.*, **101,** 6470.

[25] Carrington, Jr., T., Halonen, L., and Quack, M., 1987, *Chem. Phys. Lett.*, **140,** 512.

[26] Dübal, H.-R., Ha, T.-K., Lewerenz, M., and Quack, M., 1989, *J. chem. Phys.*, **91,** 6698.

[27] Iung, C., and Leforestier, C., 1989, *J. chem. Phys.*, **90,** 3198.

[28] Iung, C., and Leforestier, C., 1992, *J. chem. Phys.*, **97,** 2481.

[29] Quack, M., 1990, *Ann. Rev. phys. Chem.*, **41,** 839.

[30] Hollenstein, H., Marquardt, R., Quack, M., and Suhm, M. A., 1994, *J. chem. Phys.*, **101,** 3588.

[31] Pochert, J., Quack, M., Stohner, J., and Willeke, M., 2000, *J. chem. Phys.*, **113,** 2719.

[32] Beil, A., Luckhaus, D., Marquardt, R., and Quack, M., 1994, *Faraday Discuss. chem. Soc.*, **99,** 49.

[33] Lin, H., Yuan, L. F., He, S. G., and Wang, X. G., 2000, *Chem. Phys. Lett.*, **332,** 569.

[34] Lin, H., Bürger, H., He, S. G., Yuan, L. F., Breidung, J., and Thiel, W., 2001, *J. phys. Chem.* A, **105,** 6065.

[35] Lin, H., Bürger, H., Mkadmi, E. B., He, S. G., Yuan, L. F., Breidung, J., Thiel, W., Huet, T. R., and Demaison, J., 2001, *J. chem. Phys.*, **115,** 1378.

[36] Bürger, H., and Ruff, A., 1970, *Spectrochim Acta*, **26,** 1449.

[37] Campargue, A., Stoeckel, F., and Terrile, M. C., 1986, *Chem. Phys.*, **110,** 145.

[38] Cheng, J. X., Lin, H., Hu, S. M., He, S. G., Zhu, Q. S., and Kachanov, A., 2000, *Appl. Opt.*, **39,** 2221.

[39] Hu, S. M., Lin, H., He, S. G., Cheng, J. X., and Zhu, Q. S., 1999, *Phys. Chem. chem. Phys.*, **1,** 3727.

[40] Rothman, L. S., Rinsland, C. P., Goldman, A., Massie, S. T., Edwards, D. P., Flaud, J. M., Perrin, A., Camy-Peyret, C., Dana, V., Mandin, J. Y., Schroeder, J., McCann, A., Gamache, R. R., Wattson, R. B., Yoshino, K., Chance, K. V., Jucks, K. W., Brown, L. R., Nemtchinov, V., and Varanasi, P., 1998, *J. Quantum Spectrosc. Radiat. Transfer*, **60,** 665.

[41] He, S. G., Zheng, J. J., Hu, S. M., Lin, H., Ding, Y., Wang, X. H., and Zhu, Q. S., 2001, *J. chem. Phys.*, **114,** 7018.

[42] Papousek, D., and Aliev, M. R., 1982, *Molecular Vibrational-Rotational Spectra* (Amsterdam: Elsevier).

[43] Bernheim, R. A., Lampe, F. W., O'Keefe, J. F., and Qualey, III, J. R., 1983, *Chem. Phys. Lett*, **100,** 45.